ADAPTIVE GRID MULTIHOP ROUTING PROTOCOL (AGMRP) FOR A HOMOGENEOUS WSN USING SPECTRAL GRAPH PARTITIONING TECHNIQUE

Z.M Abubakar[1], E.A Adedokun[2], M.B Mu'azu[3] and I.J Umoh[4]
Department of Computer Engineering, Ahmadu Bello University Zaria, Nigeria
[1]xeenabu@yahoo.com, [2]wale@abu.edu.ng, [3]mbmuazu@abu.edu.ng,
[4]ime.umoh@gmail.com.

Keywords: –
Clustering
Energy consumption
Network lifetime
Routing protocols
WSN

Article History: –
Received: July, 2020.
Reviewed: August, 2020
Accepted: September, 2020
Published: September, 2020

ABSTRACT

Energy limitation is a major constraint affecting the performance of a WSN due to the limited energy of the nodes. The sensor nodes are mostly battery-powered and are deployed in remote or hostile surroundings, whereby it is difficult to recharge or replace the batteries regularly. Thus, hindering their ability to carry out their functions efficiently. As such, reducing energy consumption and prolonging the lifetime of the nodes becomes necessary. In this paper, an energy-efficient routing algorithm was developed utilizing the spectral graph-partitioning technique based on Normalized cut (Ncut) that optimally partitioned the network into clusters (grids). An unequal clustering mechanism for mitigating the hotspot problem was incorporated into the routing algorithm. The algorithm was implemented in MATLAB R2018a and was evaluated using network lifetime, energy consumption, and some alive nodes as performance metrics. Simulations were carried out in two scenarios, and results showed that AGMRP outperformed other algorithms.

1. INTRODUCTION

A homogeneous Wireless Sensor Network (WSN) is a network that has nodes with the same storage, energy, processing and communication capabilities. The sensor nodes perform sensing, processing, and wireless communication [15]. They are equipped with low battery power and are often deployed in a hostile environment [5]. Energy limitation is one of the key constraints affecting the performance of a WSN, because of the limited energy of the nodes. The battery-powered nature and deployment mostly in a hostile environment whereby it is difficult to replace or recharge the batteries hinder their ability to carry out function efficiently. Design of energy-efficient routing protocols, regular battery replacement, and energy harvesting from natural sources are some of the ways employed to alleviate the effect of energy limitation in WSNs [6]. Harvesting natural sources are totally climatic-dependent; their energy source is potentially sporadic [10] [2] and, therefore seems unreliable. The use of energy harvesting often requires management schemes for efficient usage of the harvested energy, hence becomes expensive. The management schemes are meant to overcome the energy output insufficiency due to temporal variation in supply [3]. Due to the deployment of sensor nodes mostly in a hostile environment where it is difficult to replace the battery, and the high cost and unreliability for energy harvesting; designing efficient routing protocols seems to be more preferable. In designing routing protocols, clustering methods have been employed to tackle problems of limited energy of the nodes [31] [7]. The process optimizes energy consumption, aggregate data, and enhances network lifetime [24]. A crucial goal in WSN for efficient design of routing protocol is minimizing the network power consumption, which comprises reducing the overall energy exhausted in the network, the amount of data transmission, and balancing the energy load among nodes in the network [5].

Due to the distinctive features of WSNs, routing protocols are expected to have the following properties [5]:

1. **Scalability**: - The routing protocols should function in an extensive network efficiently, even with an increased amount of nodes.
2. **Efficiency**: - The routing protocols should be efficient in terms of energy and time, due to the intense energy limitation of the network and their time-dependent application scenarios.
3. **Fault tolerance**: - Sensor network should continue to be operational for quite a long time despite the failure of some nodes.

To tackle the problem of energy limitation of sensor nodes and deployment issues in a WSN, clustering methods have

been a promising alternative [31] [26] [29]. Clustering is more challenging in a homogeneous WSN because the CH nodes are selected from sensor nodes with the same energy level, storage, and processing capabilities. But in the case of a heterogeneous WSN, there are different sensor nodes, and a less energy-constraint node can be selected as the CH node. A lot of energy-efficient routing protocols have been developed for WSN. However, there is still a need to explore new ways of designing efficient protocols that will utilize the limited energy of the nodes. Therefore, this research proposed an energy-efficient routing protocol using graph partitioning technique to segment the network into clusters, in order to minimize energy consumption and balance loads among the sensor nodes with a view to extend the network lifetime. Network partitioning and cluster formation were treated as a graph-partitioning problem, and the graph was segmented using the concept of normalized cut (Ncut) proposed by [24]. The Ncut criterion measures the disconnectedness between clusters and the togetherness of sensor nodes within groups. Several parameters were considered in the selection of functional nodes to reduce the total energy required by the nodes to send messages. Reducing the overall energy consumed by the sensor network per round is a challenge in WSN, and can be attained through optimal cluster formation.

Most designs of routing algorithms in a WSN do not consider the effect of hotspot problems that may result in a network partition. Hotspot problem is a condition that often results in isolation or network partition due to unbalanced energy consumption [5] [22]. It reduces the network lifetime [32]; as such, it is a critical point of focus when considering energy efficiency in WSNs. Hotspot problem occurs in both single-hop and multi-hop communication. In addition to achieving energy efficiency in the network, it is also necessary to mitigate the hotspot problem. To address the hotspot problem, an unequal clustering mechanism was used. The grid sizes were varied based on the distance to the base station, in such a way that clusters closer to the base station have smaller dimensions than those that are farther away, to overcome the energy over-consumption around the base station.

2. RELATED WORKS

The significant results related to this research can be studied in the literature.

In [10], an energy-efficient protocol referred to as Low Energy Adaptive Clustering Hierarchy (LEACH) for wireless microsensor networks was proposed. It is the pioneer hierarchical routing protocol. To distribute the energy load evenly among the sensor nodes, randomization was used in selecting the CH node. The protocol showed significant improvement in system lifetime and reduction in energy dissipation. However, it may result in a non-uniform distribution of CH nodes and a low clustering setup due to random CH nodes selection. Moreover, the use of the single-hop transmission is not ideal for large scale WSN because nodes that are farther away from the base station tends to deplete their energy faster, resulting in hotspot problem.

In [8], a method for designing routing protocol in WSNs named Spectral Classification based on Near-Optimal Clustering was developed. The protocol was established using spectral division for segmenting the network into two different clusters. The algorithm extended network lifetime and reduced the energy consumed. However, the method cannot segment the network into any desired number of clusters. Also, the critical hotspot problem due to multi-hop routing that may cause early depletion of nodes close to the base station because of inter-cluster transmission was not addressed in the development of the protocol.

In [33], a clustering technique for WSN based on minimum hop was proposed. The minimum hop value obtained by each node was used to obtain the communication radius. The aggregated data were transferred by the CH via multi-hop transmission, using the direction of the minimum hop gradient. All the nodes knew their neighbors and thus calculated their weight. The algorithm balanced energy consumption and increased network survival time. However, the node residual energy was not considered in CH selection. Therefore, there is a high tendency that a low energy node would be chosen as CH, which might result in an energy hole problem.

In [30], a clustering-based algorithm that is energy saving for a wide-ranging WSN that reduces power consumption was developed. The protocol selected CHs considering deployment information about the node, the degree of a node, residual energy, and distance from the base station. The algorithm extended the network lifetime and improved the network coverage. However, CHs forwarded data to the base station directly using single-hop transmission, and it is not ideal for use in the large-scale network because CH nodes that are much afar from the base station are more likely to expend all their energy faster, causing network partition.

In [27], a new clustering approach for WSN that is energy-efficient and distribution independent was developed. The clustering problem was considered in both uniform and non-

uniformly distributed networks. The algorithm is a fuzzy clustering algorithm that used local decision to determine the competition radius of nodes and elect tentative and final CH nodes. They considered nodes remaining energy, node density, and distance to the base station in the selection of CH nodes. The algorithm was evaluated in four scenarios. The performance of the algorithm was experimentally evaluated and has shown better results compared to some existing algorithms. However, the CH nodes were randomly selected before screening them for final selection based on competition range and rank, and random selection might result in the selection of a low energy node in a cluster as CH.

In [12], an enhanced protocol that adopts multi-hop routing for a homogeneous WSN was proposed. The protocol divided the CH nodes into internal and external CHs depending on their distance to the base station. Internal CH served as relay nodes to external CH nodes. The protocol balanced the network energy consumption and efficiently prolonged its lifetime. However, the developed protocol does not consider nodes' energy level during the process of CH selection, which can result in the problem of the energy hole when a sensor node with lesser energy is selected as CH.

In [1], a fuzzy-based unequal clustering algorithm named FUCA was proposed. The algorithm formed unequal clusters, so as to evenly distribute the energy consumed by the nodes. Using fuzzy logic approach, the CHs were selected. Nodes residual energy, nodes degree, and distance from the base station were used as the input variables, and the output variables were competition radius and rank. The algorithm was evaluated in different scenario consisting of different number of sensor nodes and position of base station, and has shown good result. However, random selection of preliminary CHs might result in selection of a low energy node as a CH in a cluster, thereby resulting in energy hole problem.

In [13], a routing algorithm for WSN based on grid clustering that adopts a multi-hop mode of transmission was developed. The entire area was partitioned into uneven grids (clusters). Sensor nodes energy with their locations and levels were combined to optimize the electoral process of selecting functional nodes. The routing protocol showed significant enhancement in network lifetime, scalability, and energy consumption with comparison to other protocols. However, the sizes of the grid signifying clusters were defined at the initialization stage irrespective of the distribution of sensor nodes. Therefore, optimal cluster formation was not guaranteed.

In [25], a clustering algorithm for WSN using Graph Partitioning was developed. They proposed a novel two-level hierarchical partitioning method for WSN that partitioned the system into clusters. In their approach, each cluster has a leader called CH that aggregates data within its cluster and forwards it to a super leader (leader of all CHs). The keen leader aggregated data from all CH nodes and transmitted them to the base station. The super leader was elected from among the CH nodes. Simulation results showed improvement in network efficiency and scalability. However, using single-hop routing to forward data directly from all CHs to the super leader CH node is not ideal for the large-scale network because the CHs that are further away might deplete their energy faster. Also, re-electing super CH node from among the CH nodes might result in more overheads.

It is evident from the literature reviewed above that numerous researches have been done on reducing energy consumption in a WSN. Cluster formation, CH selection, the establishment of an appropriate route to the base station, and hotspot problems are significant challenges faced in the design of clustering algorithms for WSN. Quite some researchers conducted research using different approaches to design a routing protocol for WSN but did not consider addressing some of the challenges mentioned above. To address the issues of clustering and CH selection, inter-cluster transmission, and hotspot problem associated with most of the reviewed literature, this research used a spectral-based technique to segment the network into clusters optimally, reduced overhead of CH nodes by introducing CM nodes in each cluster to aid in inter-cluster data transmission to the base station, established appropriate multi-hop route for inter-cluster communication and addressed hotspot problem due to multi-hop routing using unequal clustering mechanism.

3. SPECTRAL CLUSTERING ALGORITHM

Spectral clustering is a class of graph clustering algorithm that partitions a graph using information from the eigenvalues and eigenvectors of their adjacency matrix [23][20]. Reformulating the problem of clustering using graph can be stated as finding a split of a chart so that edges between groups that are the same are assigned a low weight (depicting dissimilarity between points in different clusters), and those within the same group are given high value (depicting similarity between points within the same set). Spectral graph partitioning uses the second eigenvector of a

graph's Laplacian to partition the chart and has been proved [28] to guarantee an approximate to optimal cut.

Laplacian matrix is the difference between the diagonal matrix of a graph and the adjacency matrix denoted by [34]:

$$L=D-A \quad (1)$$

Where L represents graph Laplacian matrix; D represents a diagonal matrix indicating the degree of the nodes, and A is the adjacency matrix representing a measure of similarity between nodes.

The degree (d_i) of a vertex (i) is defined as the sum of weights of the edges attached to it [14][18][17] as:

$$di = \sum_{j=1}^{n} Wij \quad (2)$$

Where di denote the degree of a vertex, i and Wij denote the weight of edges connecting the nodes.

3.1 Normalized Cut (Ncut)

The Ncut is a square measure of dissociation between subdivisions of a graph that is obtained by summing the ratio of the cut value of each partition to the total weights of nodes in each section [28]. In a graph, the perfect cut minimizes the Ncut amount [16]. To partition a graph into two separate parts A and B, the edges that connect the different parts are removed [18]. It is represented by:

$$\text{Cut (A, B)} = \sum_{i\epsilon A, j\epsilon B} e_{ij} \quad (3)$$

Where e_{ij}represents the number of edges connecting parts A and B.

Cut value is the measure of variation between parts A and B, which is the aggregate of all the edge weights between nodes in part A to nodes in part B.

Ncut criterion avoids the unusual bias of segmenting smaller points by computing the cut based on the fraction of total connections of edges to all nodes in the graph, in preference to computing based on only the total weights of edges connecting the two partitions as in minimum cut criterion [28]. The Ncut is denoted by [35]:

$$\text{Ncut(A,B)} = \frac{cut\ (A,B)}{vol\ (A)} + \frac{cut\ (A,B)}{vol\ (B)} \quad (4)$$

Where cut (A, B) represents the aggregate of weights between nodes in part A and nodes in part B, that is, the number of edges crossing the partition going from one cluster to another; vol (A) represents the sum of all weights from nodes in A, that is the number of edges originating from the node within cluster A; and vol (B) represents the sum of all weights from nodes in B, that is the number of edges originating from the node within cluster B.

Ncut considers inter-cluster connections, as well as intra-cluster connections. To obtain optimal bi-partition, it has been proved in [28] that the second smallest eigenvector of generalized eigensystem is the real solution to the problem of normalized cut.

3.2 Energy Consumption Model

The model for radio energy dissipation used in computing the energy dissipation in the wireless transmission is illustrated in Figure 1.

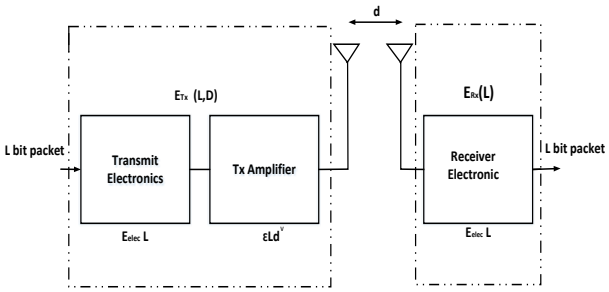

Figure 1. Radio Energy Dissipation Model [9]

In this model, energy is used by the transmitting/receiving circuitry and power amplifier. The amount of energy consumed in conveying L-bits message over a distance d is represented by $E_{Tx}(L,d)$ and that consumed in receiving L-bit message is represented by $E_{Rx}(L)$. The radio (transmit) electronics and power amplifier is powered by the expended energy from the transmitter, while the expended energy from the receiver powers the radio (receive) electronics [19]. The energy consumption rate for sending 1-bit data from the sender node S_i to receiver node S_j is denoted by [14]:

$$\begin{cases} V_i = \begin{cases} a_o + P_1 \times d\ (S_i\ , S_j\ )^2; & d\ (S_i\ , S_j) < d_o \\ a_o + P_2 \times d\ (S_i\ , S_j\ )^4; & d\ (S_i\ , S_j) \geq d_o \end{cases} \\ V_j = a_o \end{cases} \quad (5)$$

Where V_i denote the energy consumption for sending 1-bit data; V_j denote the energy consumption for receiving 1-bit data; a_o denote energy consumption of transmitting circuit; $P_1$and P_2 denote control parameters of the transmitting amplifier; $d\ (S_i, S_j)$ denote geometry distance between the transmitting node S_i and the receiving node S_j ; and d_o denote the threshold distance.

The control parameter P_1 represents E_{fs}, which denotes the amplifier energy in a free space model and P_2 represents E_{mp}, which denotes the amplifier energy in a multipath channel model.

Free space or multipath fading channel models are used considering the distance between the transmitter and the receiver. The open space model is used if the spacing d is less compared to a threshold distance d_o while a multipath fading model is used when the distance is greater than the threshold distance d_o [13][12]. The threshold distance is defined as [13]:

$$d_o = \sqrt{\frac{E_{fs}}{E_{mp}}} = \sqrt{\frac{P_1}{P_2}} \quad (6)$$

4. ADAPTIVE GRID MULTIHOP ROUTING PROTOCOL (AGMRP)

The following are the assumptions made for the system model:

1. The network is a square field, which comprises randomly generated nodes and a base station.

2. The sensor nodes are homogenous and energy-constrained.

3. The nodes and base stations are assumed to be static.

4. The base stations are powerful than the nodes and are connected to a replenished power.

5. The network is supposed to have perfect data transmission.

For evaluation, we perform a simulation of our protocol in a realistic setting. The simulation parameters are given in Table 1.

The simulation was carried out using two network regions: 200m × 200m and 400m × 400m, with base station coordinates (100m, 200m) and (200m, 400m), respectively.

The nodes were randomly deployed in the sensing area. The base station broadcasted hello message to all the sensor nodes at a particular power level, and based on the RSS; each sensor node computed its approximate distance to the base station. The Euclidean distance was calculated using:

$$d_{SiB} = \sqrt{(x_{Si} - x_{BS})^2 + (y_{Si} - y_{BS})^2} \quad (7)$$

Where d_{SiB} represent the distance from the sensor node i to the base station; x_{Si}, y_{Si} are coordinates of sensor node i and x_{BS}, y_{BS} are coordinates of the base station. $i = 1,2,3, \ldots\ldots\ldots\ldots N$

Table 1. Simulation Parameters

Parameter	Value
Length of sensor field (M)	200m and 400m
Number of sensor nodes (N)	400
Base station Coordinate	(100m, 200m) and (200m, 400m)
The initial energy of nodes (E_o)	0.5J
Message size	800 bits
$E_{elec}(a_0)$	50nJ/bit
E_{fs} (P_1)	10pJ/bit/m^2
E_{mp} (P_2)	0.0013pJ/bit/m^4

This helps them to determine the suitable power level to use in communicating with the base station.

An imaginary ellipse was formed centered around each sensor node, with its central axis equal to the length of the field and minor axis similar to $1/4$ of the width of the sensor field. The nodes s_i and s_j are adjacent if there is an intersection between their ellipses. The adjacency matrix can be defined mathematically as:

$$A_{ij} = \begin{cases} 1, & \frac{(x_{si} - x_{Sj})^2}{a^2} + \frac{(y_{si} - y_{Sj})^2}{b^2} <= 1 \\ 0, & \text{Otherwise} \end{cases} \quad (8)$$

Where (x_{Si}, y_{Si}) and (x_{Sj}, y_{Sj}) are coordinates of sensor nodes s_i and s_j respectively; a and b are the length of the major and minor axis of the ellipse surrounding the nodes respectively; s_i represents sensor node i and s_j represents sensor node j.

Sensor nodes s_i & s_j are adjacent if the condition in equation (9) was satisfied; otherwise, they are not contiguous.

$$\frac{(x_{si} - x_{Sj})^2}{a^2} + \frac{(y_{si} - y_{Sj})^2}{b^2} <= 1 \quad (9)$$

Figure 2 shows a diagrammatic representation of two nodes s_i & s_j with intersecting ellipse.

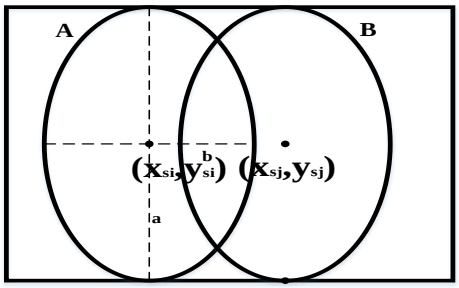

Figure 2. Sensor Nodes Intersecting Ellipse

In Figure 2, the ellipse for the sensor node s_i is labeled as A and that of sensor node s_j is labeled as B. The figure shows a representation of the coordinates of two intersecting nodes with the axis length. Using the competition ellipse of sensor nodes, the adjacency matrix of the graph was formed.

A ε $R^{N\times N}$ denote the adjacency matrix of the graph G

After obtaining the adjacency matrix, the degree of nodes was computed. Using the degree of the sensor nodes, the diagonal matrix was formed.

D ε $R^{N\times N}$ represents the diagonal matrix of graph G representing the degree of nodes. The degree of the nodes is represented by:

$$d_i=\sum_{j\in v} A_{ij} \quad (10)$$

Where d_i denotes the number of links from sensor node i to some other node j.

The graph Laplacian matrix was obtained using equation (1).

The base station constructed the graph that corresponded to the WSN. The network was represented by an undirected graph G (V, E): Where V represents, sensor nodes (set of vertices), and E represents a set of edges that links two sensor nodes within the same ellipse.

After obtaining the graph Laplacian matrix, the eigenvalues and corresponding eigenvectors were calculated. The eigenvector that corresponded to the second smallest eigenvalue was determined and sorted in ascending order. At each point, the Ncut value was computed. The point with the minimum Ncut indicating the best cut was determined. The graph was split at the point with the minimum Ncut. The chart was recursively repartitioned until the optimal number of partitions was obtained. The pseudo-code for the spectral clustering algorithm is as shown:

ALGORITHM: Spectral graph partitioning using Ncut
Input: Adjacency matrix A
Output: Graph partitions
Compute D = diag(deg (A)); //
Diagonal matrix of the degrees of the matrix A
Compute L = D – A; //
Laplacian matrix
Solve for second smallest eigenvector:
Normalized cut: Lx= λDx;
Sort the second smallest eigenvector x_2
Calculate Normalized cut
Split graph into partitions at the minimum Ncut

Figure 3 shows the pictorial representation of column-wise partitions and grids (clusters).

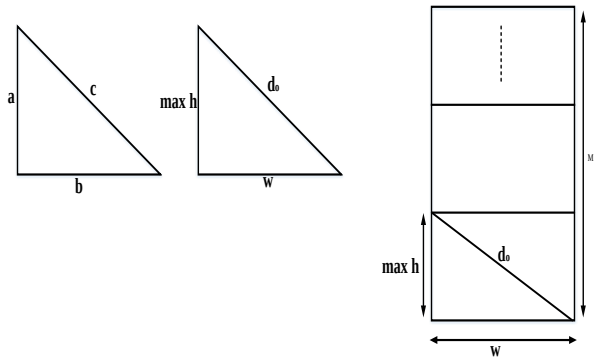

(a) (b) (c)

Figure 3. Pictorial Representation of Partition and Grids

The computation of grid height in each partition using the concept of the Pythagoras theorem is pictorially shown in Figure 3.
From Figure 3.3a,

$$c^2 = a^2 + b^2$$
$$a^2 = c^2 - b^2$$
$$a = \sqrt{c^2 - b^2}$$

Comparing Figure 3.3a with Figure 3.3b and 3.3c; a ≡ $maxh$, $b \equiv w$, and c ≡ d_o. The maximum height required for a grid in each partition referred to as maxh, is computed using:

$$\text{maxh} = \sqrt{d_o^2 - w^2} \quad (11)$$

The number of grids per column (n) referred to as the grid count is given by:

$$\text{Gridcount (n)} = \text{Ceil } (M/\text{maxh}) \quad (12)$$

Where M = length of the sensor field and maxh = maximum height of the grid. The height of the grids (h) in each partition (column) was calculated using:

$$\text{Height of grid (h)} = M/n \quad (13)$$

The threshold distance (d_0) is represented by:

$$\text{Threshold distance } (d_0) = k\text{M} \quad (14)$$

Where k = 0.45

The partitions obtained were column-wise. The number of sensor nodes per column, and the column width (w) were obtained. The maximum grid height was computed using the

concept of Pythagoras theorem, as shown in equation (11). It was assumed that in each grid (cluster), the distance between any two communicating nodes is less than d_o (i.e $d < d_o$). Therefore, in computing the height of each grid, the diagonal was chosen to be d_o because it is the maximum distance between two communicating nodes. As such, only the free space model was used in computing the energy consumed for intra-cluster communication, thereby minimizing energy consumption.

Finally, the partitions (columns) were further divided into grids signifying clusters. To avoid the hotspot problem that may occur due to multi-hop routing, the grid sizes were varied based on the distance to the base station. In each partition with an odd number of grids (grid count), the middle grid was assigned the value of the computed height (h) in equation (13). Then, the grid sizes above it closer to the base station were decreased by a fraction of the height, while those below it was increased. But, for an even number of grids (grid count) in a partition, the number of grids were divided into two (upper and lower), and the value of h was decreased by a fraction for the upper half closer to the base station and increased for the lower half farther away from the base station.

Suppose the grid count (n) that is the number of grids in each partition is 5. The grid sizes were varied, as shown in Figure 4.

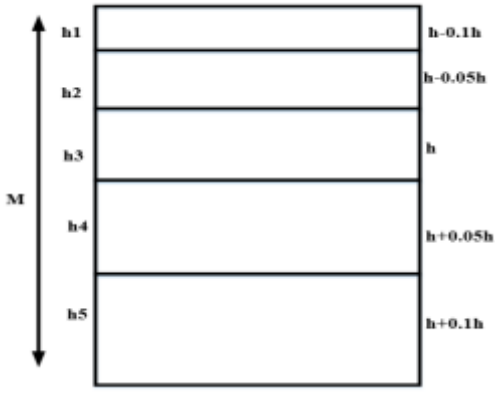

Figure 4. Varying of Grid Size

Figure 4 shows a representation of grid size computation in each partition to avoid the hotspot problem.

$$M = h_1 + h_2 + h_3 + h_4 + h_5 \quad (15)$$

M = (h – 0.1h) + (h – 0.05h) + h + (h + 0.05h) + (h + 0.1h)

= h – 0.2h + h - 0.1h + h + h + 0.1h + h + 0.2h

= h + h + h + h + h

Therefore, M = 5h = nh (16)

Equation (15) was derived from Figure 4. From equation (13), it can be observed that the length of the field was equal to the number of grids in a partition multiplied by the calculated height (h) as shown in equation (16).

To develop the functional node selection algorithm, the CM and CH nodes were selected as follows:

1. CM selection:

Using residual energy and sensor nodes distance to the base station, CM nodes were chosen in each cluster. The distance from the node of each cluster to the base station was computed using:

$$d_{ScB} = \sqrt{(x_{Si} - x_{BS})^2 + (y_{Si} - y_{BS})^2} \quad (17)$$

Where d_{ScB} represents the distance from the sensor node in each cluster to the base station; x_{Si} and y_{Si} represents x and y coordinates of node i; x_{BS} represents x-coordinate of the base station and y_{BS} represents the y-coordinate of the base station. The normalized energy level and normalized distance to the base station were calculated for each node i using equations (18) and (19), respectively.

$$N_{e_{Si}} = \frac{E_{Si}}{\max\limits_{j \in C} E_{Sj}} \quad (18)$$

$$N_{d_{SiB}} = \frac{d_{SiB}}{\max\limits_{j \in C} d_{SjB}} \quad (19)$$

Where $N_{e_{Si}}$ represents the normalized energy of sensor node i; E_{Si} represents residual energy of sensor node i; $\max\limits_{j \in C} E_{Sj}$ represents the energy of the node with the maximum residual energy within the cluster; $N_{d_{SiB}}$ represents the normalized distance of node i to the base station; d_{SiB} represents the distance of the sensor node i to the base station, and $\max\limits_{j \in C} d_{SjB}$ represents the distance of the node with the maximum distance to the base station. The weighting for each sensor node was computed using:

$$W_i = N_{e_{Si}} \times (1 - N_{d_{SiB}}) \quad (20)$$

Where W_i represents the weight of sensor node i.
After computing weights for each sensor node, the sensor node with maximum weighting was selected as CM in each cluster. It is defined mathematically as

$$CM_c = \max(W_i) \quad (21)$$

Where CM_c represents the CM node in each cluster.

2. CH Selection:

CH nodes were selected using residual energy and distance of sensor nodes to the cluster centroid. For each cluster, the centroid was obtained using:

$$x_c = \frac{\sum_{i=1}^{N} x_{Si}}{N_c} \quad (22)$$

$$y_c = \frac{\sum_{i=1}^{N} y_{Si}}{N_c} \quad (23)$$

Where x_c and y_c represents x and y coordinates of the cluster centroid; N_c represent a number of nodes in the cluster; i and j are indexes representing sensor nodes $i \in (1, \ldots \ldots \ldots N)$ and $j \in (1, \ldots \ldots \ldots N)$ respectively. In a cluster, the distance from each sensor node (S_i) to the cluster centroid was calculated using:

$$d_{SiC} = \sqrt{(x_{Si} - x_c)^2 + (y_{Si} - y_c)^2} \quad (24)$$

Where d_{SiC} represents the distance from sensor node i (s_i) to cluster centroid. The normalized energy level and normalized distance from centroid were calculated for each sensor node S_i in a cluster using:

$$N_{e_{Si}} = \frac{E_{Si}}{\max\limits_{j \in C} E_{Sj}} \quad (25)$$

$$N_{d_{SiC}} = \frac{d_{SiC}}{\max\limits_{j \in C} d_{SjC}} \quad (26)$$

Where $N_{d_{SiC}}$ is the normalized distance of node i to cluster centroid and $\max\limits_{j \in C} d_{SjC}$ represents the node within the cluster with the maximum distance to the cluster centroid. The weighting for each sensor node was computed using:

$$W_i = N_{e_{Si}} \times (1 - N_{d_{SiC}}) \quad (27)$$

After computing weights for each sensor node, the sensor node with maximum weighting was selected as CH in each cluster. It is defined mathematically as:

$$CH_c = \max(W_i) \quad (28)$$

Where CH_c represents the CH node in each cluster.

A multi-hop routing algorithm between CM nodes of each cluster was developed as follows: Each sensor node sensed data and transmitted the data to their respective CHs. The sensed data was aggregated by the CHs and forwarded to their CM nodes. The CM nodes near the base station transmitted data to it directly; otherwise, they transmitted via the next-hop CM node. The Flowchart showing multi-hop routing and data transmission step is shown in Figure 5.

The steps followed to transmit data to the base station are illustrated in Figure 5.

4.1 Simulation Results

In this work, the connectedness between nodes was modeled by using a "1" if nodes were within the range of each other or a "0" if they were not. The network was represented as a graph in the form of an Adjacency matrix. The Adjacency matrix was formed after identifying those sensor nodes that were adjacent using an ellipse formed around each node. After obtaining the adjacency matrix, the degree of nodes was computed. The diagonal matrix was then developed using the degree of nodes. The graph Laplacian matrix was then calculated.

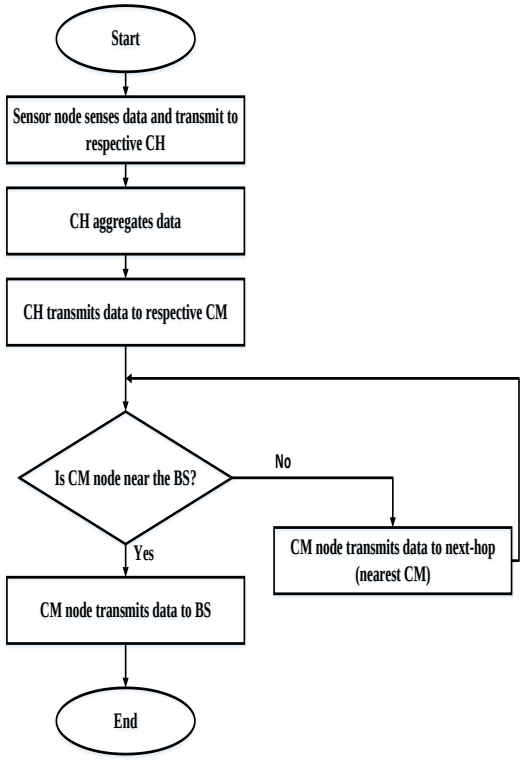

Figure 5. Flowchart of Multi-hop and Data Transmission Step

4.1.1 First scenario of AGMRP

After obtaining the graph Laplacian matrix, the eigenvalues and eigenvectors were computed. The eigenvector that corresponded to the second smallest eigenvalue was determined and permutated. At each point, the Normalized cut (Ncut) value was calculated, and the point with the minimum Ncut was determined.

The Ncut achieved optimal clustering, which prolonged the network lifetime by balancing loads among the sensor nodes. The graph was split at the point with the minimum Ncut as shown in Figure 4.5

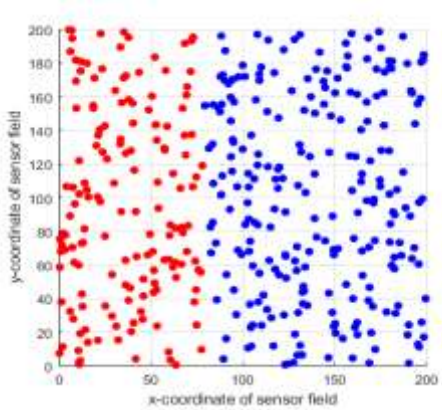

Figure 6. Splitting Point with Minumun Ncut Value for Scenario1

In Figure 6, the splitting point of the graph that has the minimum Ncut value representing the best cut in the first scenario is shown. From the plot, the minimum Ncut amount indicated the position of optimal bi-partitioning. Repeating the process also repartitioned the larger part of the graph. After recomputing and permutating for the larger part, the chart was split at the point with the minimum Ncut, as shown in Figure 7.

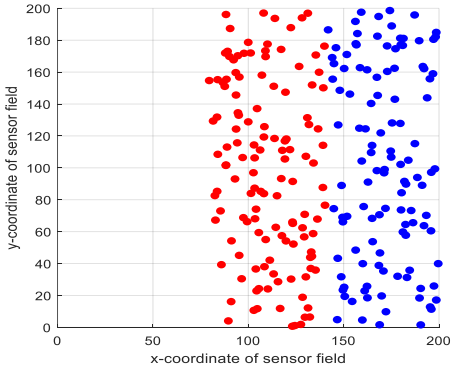

Figure 7. Splitting Point with Minimum Ncut for the Larger Partition in Scenario1

In Figure 7, the splitting point of the larger part of the graph for the first scenario is shown. The optimal partitions obtained by the algorithm is shown in Figure 8.

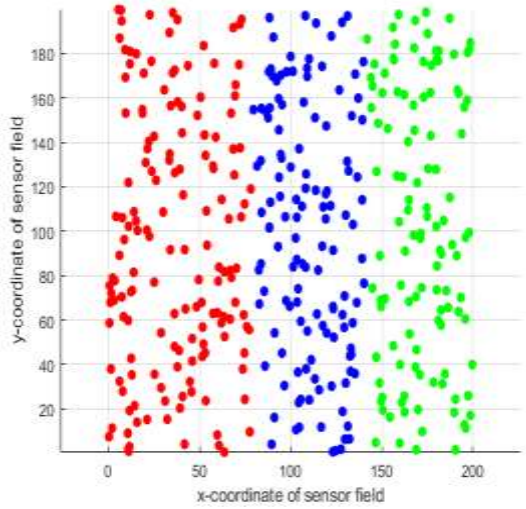

Figure 8. Optimal Partitions Obtained in Scenario1

Figure 8 shows the partitions obtained by the developed algorithm for the first scenario. The sections were divided into grids signifying clusters, as shown in Figure 9.

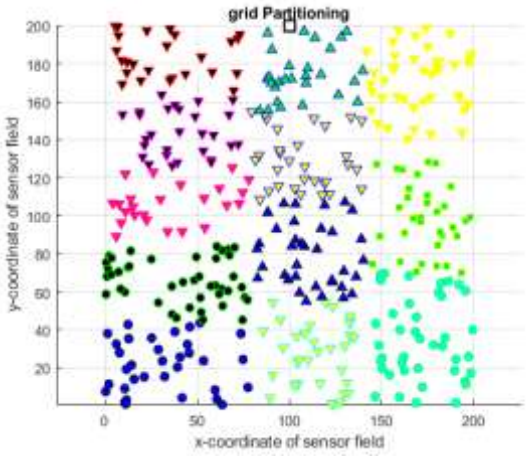

Figure 9. The Grid Partitioning for Scenario1

In Figure 9, the grids obtained in each column after the partitioning of the network in the first scenario are shown. The sensor nodes were distributed uniformly over the sensing area. It can be observed that by using the spectral graph partitioning technique, optimal clustering was achieved.

4.1.2 Second scenario of AGMRP

After obtaining the graph Laplacian matrix, the eigenvalues and eigenvectors were computed. The eigenvector that

corresponds to the second smallest eigenvalue was determined and permutated.

At each point, the Ncut value was calculated, and the point with the minimum Ncut was determined. The graph was split at the point with the minimum Ncut, as shown in Figure 10.

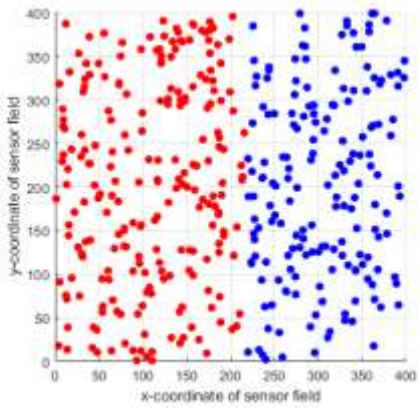

Figure 10. Splitting Point with Minimum Ncut Value for Scenario2

In Figure 10, the splitting point of the graph that has the minimum Ncut value representing the best cut in the second scenario is shown. The first partition of the chart was repartitioned by repeating the process.

At each point, the Ncut value was computed, and the point with the minimum Ncut was determined.

The graph was split at the point with the minimum Ncut, as shown in Figure 11.

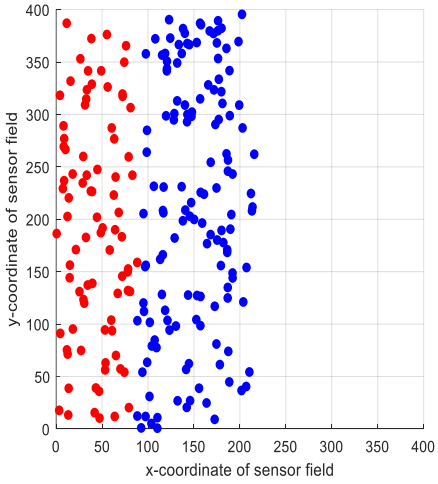

Figure 11. Splitting point with Minimum Ncut for the First Partition in Scenario2

In Figure 11, the splitting point of the first partition of the graph for the second scenario is shown. The second partition of the graph obtained in Figure 10 was also repartitioned.

The graph was split at the point with the minimum Ncut, as shown in Figure 12.

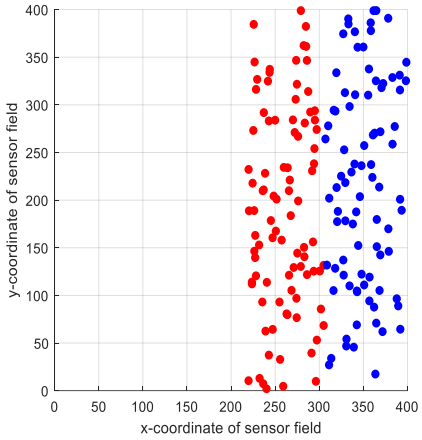

Figure 12. Splitting point with Minimum Ncut for the Second Partition in Scenario2

In Figure 12, the splitting point of the second partition of the graph that has the minimum Ncut value for the second scenario is shown. The optimal partitions obtained by the algorithm are shown in Figure 13.

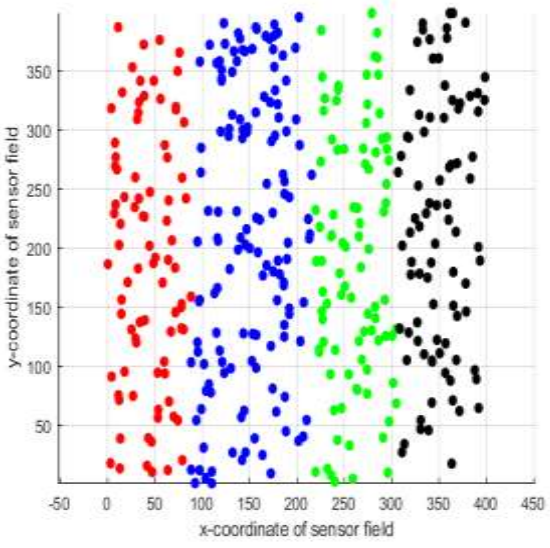

Figure 13. Optimal Partitions Obtained for Scenario2

Figure 13 shows the partitions obtained by the developed algorithm for the second scenario. The partitions were divided into grids signifying clusters, as shown in Figure 14.

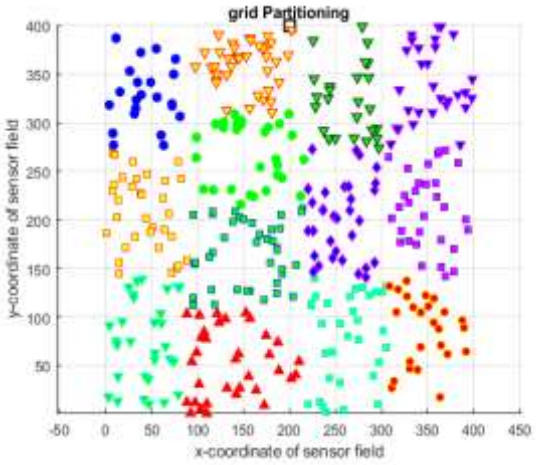

Figure 14. The Grid Partitioning for Scenario2

In Figure 14, the grids obtained in each column after the partitioning of the network in the second scenario are shown. The nodes were distributed uniformly over the sensing area. It can be observed that by using the spectral graph partitioning technique, optimal clustering was achieved.

LEACH, FUCA, and EEMRP protocols were replicated and compared with the developed AGMRP protocol. The performances were evaluated as follows:

1. Network lifetime

The round of death occurrence for the 1st, 100th, 200th, 300th and 400th node in both scenarios are as follows:

a) First Scenario

The 1st node death in LEACH, FUCA, EEMRP, and AGMRP occurred at 493rd, 548th, 539th, and 706th round, respectively. The 100th node death in LEACH, FUCA, EEMRP, and AGMRP occurred at 522nd, 597th, 799th, and 819th round, respectively. The 200th node death in LEACH, FUCA, EEMRP, and AGMRP occurred at 529th, 612th, 815th, and 859th round, respectively. The 300th node death in LEACH, FUCA, EEMRP, and AGMRP occurred at 538th, 623rd, 836th, and 891th round, respectively. The 400th node death in LEACH, FUCA, EEMRP, and AGMRP occurred at 544th, 629th, 883rd, and 916th round, respectively.

The end of the 1st, 100th, 200th, 300th and 400th nodes and round of occurrence in LEACH, FUCA, EEMRP, and AGMRP are shown in Figure 15.

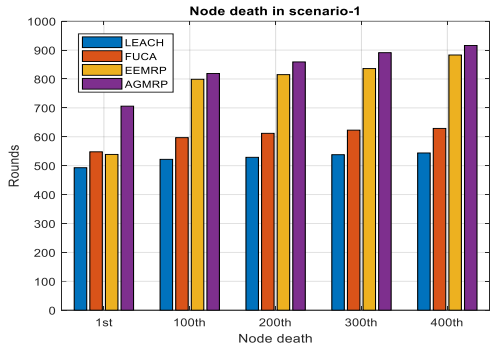

Figure 15. Bar chart of Node death in Scenario1

Figure 15 is a bar chart showing the death of 1st, 100th, 200th, 300th and 400th node. The result showed that there is an improvement in network lifetime in AGMRP compared to the other protocols because the time of occurrence of the First Node Death (FND) was delayed. The result showed that network lifetime had been improved by 43.21%, 28.83%, and 30.98% compared to LEACH, FUCA, and EEMRP, respectively.

b) Second Scenario

The 1st node death in LEACH, FUCA, EEMRP, and AGMRP occurred at 384th, 391st, 319th, and 627th round, respectively. The 100th node death in LEACH, FUCA, EEMRP, and AGMRP occurred at 464th, 455th, 501st, and 737th round, respectively. The 200th node death in LEACH, FUCA, EEMRP, and AGMRP occurred at 479th, 472nd, 568th, and 765th round, respectively. The 300th node death in LEACH, FUCA, EEMRP, and AGMRP occurred at 496h, 487th, 627th, and 805th round, respectively. The 400th node death in LEACH, FUCA, EEMRP, and AGMRP occurred at 505th, 493rd, 720th, and 830th round, respectively.

The death of the 1st, 100t, 200th, 300th and 400th nodes and round of occurrence in LEACH, FUCA, EEMRP, and AGMRP are shown in Figure 16.

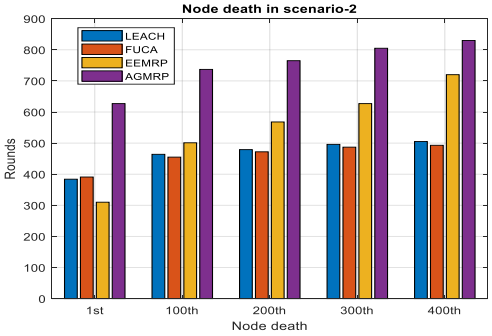

Figure 16. Bar Chart of Node Death in Scenario2

Figure 16 is a bar chart showing the death of 1st, 100th, 200th, 300th and 400th node. The result showed that there is an improvement in network lifetime in AGMRP compared to the other protocol because the time of occurrence of the First Node Death (FND) was delayed. The result showed that network lifetime had been improved by 63.28%, 60.36%, and 99.35% compared to LEACH, FUCA, and EEMRP, respectively. The reason for the low performance of EEMRP for the other algorithms in terms of FND in scenario2 was as a result of the following:

i. Scenario2 has a lower number of sensor nodes per unit area (density).

ii. EEMRP has a high number of grids for scenario2.

iii. Due to reason (i) and (ii), EEMRP has grids with very few sensor nodes, which end up been overworked as CH/ CM nodes, leading to their early death.

iv. All the other algorithms have a system of checking the minimum number of sensor nodes per cluster, which makes them perform better.

It can be observed that the 1st, 100th, 200th, 300th, and 400th node death occurred at different times in both scenarios. This is because all nodes do not consume the same amount of energy in every round due to varying distances from the base station. However, clustering and hierarchical routing protocol aim at balancing the load among sensor nodes.

2. Total energy consumption

The Total Residual Energy (TRE) and Total Energy Consumed (TEC) in all the scenarios are as follows:

a) First Scenario

The TRE in scenario 1 for LEACH, FUCA, EEMRP, and AGMRP are shown in Figure 17.

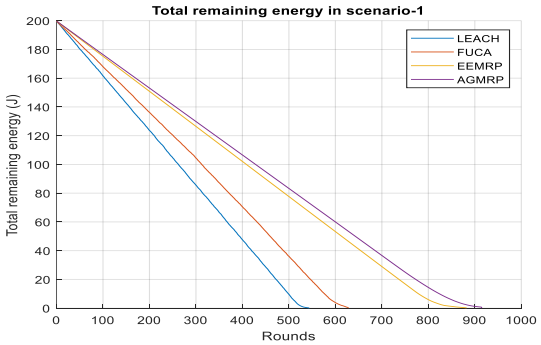

Figure 17. TRE in Scenario1

Figure 17 gives the total remaining energy in every round of transmission for LEACH, FUCA, EEMRP, and AGMRP for the first scenario. The energy decreases faster in LEACH, FUCA, and EEMRP than in AGMRP.

The TEC in scenario1 for LEACH, FUCA, EEMRP, and AGMRP are shown in Figure 18.

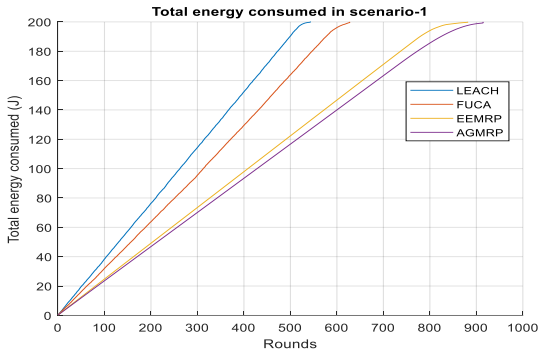

Figure 18. TEC in Scenario1

Figure 18 shows the graphical representation of the TEC versus the number of rounds for all the protocols for the first scenario. It can be seen that the TEC in AGMRP was lower at each round compared to LEACH, FUCA, and EEMRP. The energy was exhausted in LEACH, FUCA, and EEMRP between round 500 to 600, 600 to 700, and 800 to 900, respectively. This showed that AGMRP has lower energy consumption. At around 400, the result showed that energy consumption had been reduced by 38.72%, 26.82%, and 4.60% compared to LEACH, FUCA, and EEMRP, respectively.

b) Second Scenario

The TRE in scenario2 for LEACH, FUCA, EEMRP, and AGMRP are shown in Figure 19.

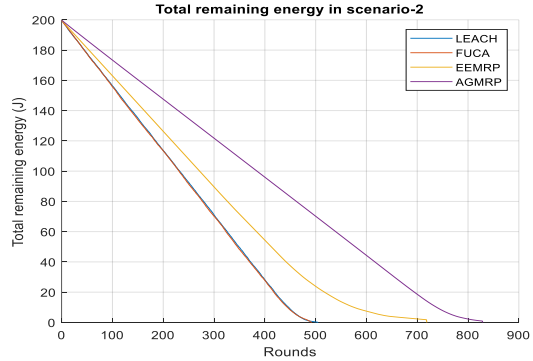

Figure 19. TRE in Scenario2

Figure 19 gives the total remaining energy in every round of transmission for LEACH, FUCA, EEMRP, and AGMRP for the second scenario. The energy decreases faster in LEACH, FUCA, and EEMRP than in the AGMRP.

The TEC in scenario2 for LEACH, FUCA, EEMRP, and AGMRP are shown in Figure 20.

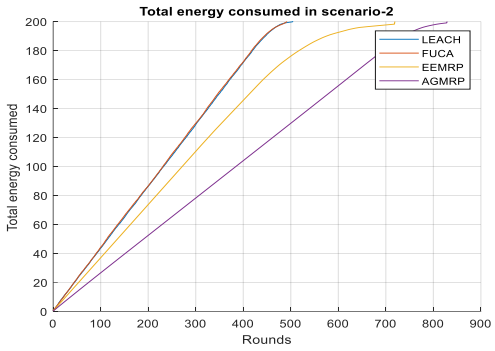

Figure 20. TEC in Scenario2

Figure 20 shows the graphical representation of the total energy consumed versus the number of rounds for all the protocols using the second scenario. It can be seen that the TEC in AGMRP was lower at each round compared to LEACH, FUCA, and EEMRP. The energy was exhausted in LEACH, FUCA, and EEMRP between round 500 to 600, 400 to 500, and 700 to 800, respectively. This showed that AGMRP has lower energy consumption. At around 400, the result showed that energy consumption had been reduced by 39.28%, 39.71%, and 28.58% compared to LEACH, FUCA, and EEMRP, respectively.

Based on the results obtained in both scenarios, it can be observed that AGMRP reduced energy consumption in the network, thereby prolonged the network lifetime.

The gradient of the TRE and TEC were approximately constant throughout. This indicates a continuous rate of sensor nodes energy depletion, which was as a result of effective load balancing among the sensor nodes.

3. Number of alive nodes

The number of active nodes in all the scenarios is as follows:

a) First Scenario

The number of alive nodes in LEACH, FUCA, EEMRP, and AGMRP is shown in Figure 21.

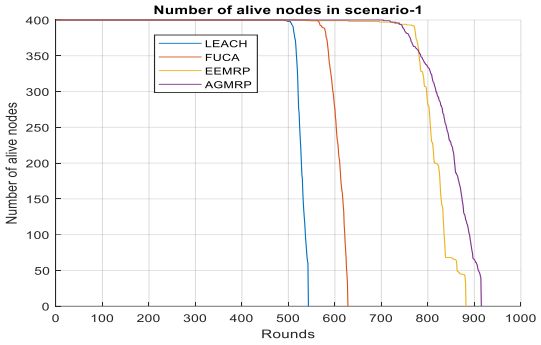

Figure 21. Number of Alive Nodes in Scenario1

The graphical representation of the number of alive nodes versus the number of rounds in the first scenario for all the protocols is shown in Figure 21. It can be seen that in LEACH, all the nodes were alive at around 0 to 492. The death of the first node occurred at about 493, and the last node death occurred at around 549. In FUCA, all the nodes were alive at around 0 to 547. The end of the first node occurred at about 548, and the last node death occurred at around 636. In EEMRP, all the nodes were alive at around 0 to 538. The end of the first node occurred at about 539, and the last node death occurred at around 882.

In AGMRP, all the nodes were alive at around 0 to 705. The death of the first node occurred at about 706, and the last node death occurred at around 915. This shows that there were more alive nodes at each round in AGMRP as a result of a balanced load among the sensor nodes. Furthermore, considering the residual energy of nodes, node density, and distance to the base station in selecting functional nodes (CH and CM) has led to a reduction in energy consumption. It thereby resulted in less number of dead nodes.

b) Second Scenario

The number of alive nodes in LEACH, FUCA, EEMRP, and AGMRP is shown in Figure 22.

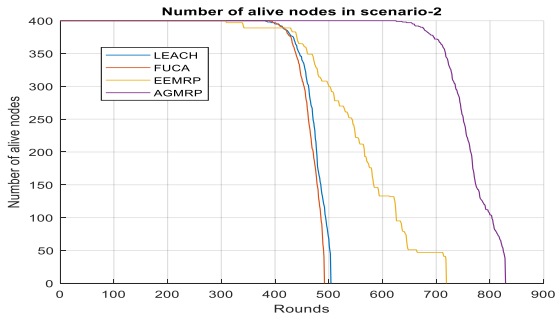

Figure 22. Number of Alive Nodes in Scenario2

The graphical representation of the number of alive nodes versus the number of rounds in the second scenario for LEACH, FUCA, EEMRP, and AGMRP is shown in Figure 22. It can be seen that in LEACH, all the nodes were alive at around 0 to 383. The death of the first node occurred at about 384, and the last node death occurred at around 506. In FUCA, all the nodes were alive at around 0 to 390. The end of the first node occurred at about 391, and the last node death occurred at around 493. In EEMRP, all the nodes were alive at around 0 to 318. The end of the first node occurred at about 319, and the last node death occurred at around 719.

In AGMRP, all the nodes were alive at around 0 to 626. The death of the first node occurred at about 627, and the last node death occurred at around 829. This shows that there were more alive nodes at each round in AGMRP as a result of a balanced load among the sensor nodes. Moreover, considering the residual energy of nodes, node density, and distance to the base station in selecting functional nodes (CH and CM) has led to a reduction in energy consumption. It thereby resulted in less number of dead nodes.

Also, the node death in AGMRP occurred more steady and gradual when compared to the other protocols. This indicated effective load balancing among the sensor nodes in AGMRP.

Based on the results obtained, it can be observed that reducing the energy consumption conserved the limited energy of the sensor nodes. Thereby extending the network lifetime.

5. CONCLUSION

In this paper, we proposed an adaptive grid multi-hop routing protocol for a homogeneous WSN using spectral graph partitioning technique, which conserved the limited energy and extended the network lifetime. As a means of validation, LEACH, FUCA, and EEMRP routing protocols were replicated and their performances compared with the developed AGMRP protocol, using network lifetime, number of alive nodes, and energy consumption as metrics. Simulation results showed that AGMRP performs better in each scenario compared to LEACH, FUCA, and EEMRP. The work indicated that optimizing the grid regions, addressing hotspot problems and considering residual energy, node density (cluster centroid), distance to the base station in functional node (CH and CM) selection have a positive effect on improving the performance of the protocol. Also, reducing the overhead of CH nodes by introducing CM nodes in each cluster aided in reducing energy consumption. The developed protocol conserved the limited energy of the nodes by reducing energy consumption through balancing the load among the sensor node, hence extended the network lifetime.

The following possible areas of further works are recommended for further research:

1. The implementation of the developed algorithm on a live WSN, to ascertain the robustness of the algorithm in a real-life scenario where path loss, various disturbances, and un-modeled non-linearity affect the system.
2. Improvement of the algorithm for a dynamic WSN, to ascertain the robustness of the algorithm in situations where the positions of the sensor nodes are active.
3. Development of a weighted communication graph based on the calculated probability of link failure estimated using Signal to Noise Ratio (SNR) for every communication link.

REFERENCES

[1] Agrawal, D., & Pandey, S. (2017). FUCA: Fuzzy-based unequal clustering algorithm to prolong the lifetime of wireless sensor networks. *International Journal of Communication Systems, Wiley online library, e3448, 1-18.*

[2] Aslam, N., Xia, K., Haider, M.T., & Hadi, M.U. (2017). Energy-aware adaptive weighted grid clustering algorithm for renewable wireless sensor networks. *Journal of Future Internet, 9, 54.*

[3] Babayo, A.A., Anisi, M.H., & Ali, I. (2017). A review of energy management schemes in energy harvesting wireless sensor networks. *Journal of Renewable and Sustainable Energy Reviews, Elsevier, 76, 1176-1184.*

[4] Balamurali, R., & Kathiravan, K. (2016). Mitigating hotspot problems in wireless sensor networks using tier-based quantification. *Journal of Cybernetics and Information Technologies, 16(1), 73-79.*

[5] Boukerche, A. (2009). A book on "Algorithms and protocols for wireless sensor networks." *University of Ottawa, Ottawa Canada. A John Wiley & Sons, Inc, Publication.*

[6] Chen, J., He, S., & Sun, Y. (2014). A book on "Rechargeable Sensor Networks Technology, Theory and Application – Introduce Energy Harvesting to Sensor Networks." *Published by World Scientific Publishing Co. Pte. Ltd.*

[7] Chen, L., Chen, Y., & Wang, Y. (2019). An improvrd spectral graph partition intelligent clustering algorithm for low-power wireless networks. *Journal of Ambient Intelligence and Humanized Computing. https://doi.org/10.1007/s12652-019-01508-7.*

[8] Elbhiri, B., ElFkihi, S., Saadane, R., & Aboutajdine, D. (2010). Clustering in wireless sensor networks based on near-optimal bi-partitions. *6th EURO-NGI Conference o Next Generation Internet, 1-6.*

[9] Engmann, F., Katsriku, F.A., Abdulai, J., Adu-Manu, K.S., & Banaseka, F. K. (2018). Prolonging the lifetime of wireless sensor networks: A review of current techniques. *In Wireless Communications and Mobile Computing, Article ID 8035065, 1-23.*

[10] Heinzelman, W.R., Chandrakasan, A.P., & Balakrishnan, H. (2000). Energy-efficient communication protocol for wireless microsensor networks. *In the Proceedings of the Hawaii International Conference on System Sciences, Jan 4-7, 1-10*

[11] Heinzelman, W.R., Chandrakasan, A.P., & Balakrishnan, H. (2002). An application-specific protocol architecture for wireless microsensor networks. *IEEE Transactions on Wireless Communications, 1(4), 660-670.*

[12] Huang, J., Ruan, D., Hong, Y., Zhao, Z., & Zheng, H. (2017). IMHRP: An improved multi-hop routing protocol for wireless sensor networks. *Journal of Physics: Conference Series 910, 012054.*

[13]. Huang, J., Hong, Y., Zhao, Z., & Yuan, Y. (2017). An energy-efficient multi-hop routing protocol based on grid clustering for wireless sensor networks. *Springer Science + Business Media, Cluster Comput 20, 3071-3083.*

[14] Jiang, C. (2016). Introduction to spectral graph theory and graph clustering. *Retrieved from http://math.uchicago.edu/~may/REU2012/REUPaper/Jiang J.pdf.*

[15] Jorio, A., El-Fkihi, S., Elbhiri, B., & Aboutajdine, D. (2015). An energy-efficient clustering routing algorithm based on geographic position and residual energy for wireless sensor network. *Journal of Computer Networks and Communications, Hindawi Publishing Corporation, Article ID 170138, 1-11.*

[16] Kapade, S.D., Khaimar, S.M., & Chaudhari, B.S. (2015). Graph partitioning based normalized cut methods. *British Journal of Mathematics & Computer Science, 5(3), 333-340.*

[17] Luxburg, U.V. (2006). A tutorial on spectral clustering. *Technical Report No. TR-149, Max Planck Institute for Biological Cybernetics.*

[18] Miller, G.L., & Tolliver, D. (2007). Graph partitioning by spectral rounding: Applications in image segmentation and clustering.

[19]Mohemed, R.E., Saleh, A.I., Abdelrazzak, M., & Samra, A.S. (2016). Energy-efficient routing protocols for solving energy hole problem in wireless sensor networks. *Journal of Computer Networks,doi:10.1016/j.comnet.2016.12.011*

[20] Mouden, Z.A., & Jakimi, A. (2020). K-eNSC: K-estimation for Normalized Spectral Clustering. *International Conference on Intelligent Systems and Computer Vision (ISCV), IEEE, 9-11 June, Fez, Morocco.*

[21] Newman, M., Watts, O., & Strogatz, S. (2002). Random graph models of social networks. *Proceedings of the National Academy of Sciences, USA, 99, 2566-2572.*

[22] Nguyen, T.T., Pan, J.S., Dao, T.K. & Chu, S.C. (2018). Load balancing for mitigating hotspot problems in wireless sensor networks based on enhanced diversity pollen. *Journal of Information and Telecommunication, 2(1), 91-106.*

[23] Nisha, U.N., & Basha, A.M. (2020). Triangular fuzzy-based spectral clustering for energy-efficient routing in wireless sensor networks. *J. Supercomputing 76, 4302-4327.*

[24] Rostami. A.S., Badkoobe, M., Mohanna, F., Keshavarz, H., Hosseinabadi, A.R., & Sangaiah, A.K. (2018). Survey on clustering in heterogeneous and homogenous wireless sensor networks. *Journal of Supercomputing, 74(1), 277-323.*

[25] Salman, S., & Ali, H.M. (2019). Efficient clustering of the wireless sensor network by spectral graph partitioning. *International Conference on Intelligent Technologies and Applications INTAP2018, CCIS 932, 698-710, Springer.*

[26] Sambo, D.W., Yenke, B.O., Forster, A., & Dayang, P. (2019). Optimized clustering algorithms for large wireless sensor networks: A review. *MDPI – Sensors, 19, 322.*

[27] Sert, S.A., Bagci, H., & Yazici, A. (2015). MOFCA: Multi-objective fuzzy clustering algorithm for wireless sensor networks. *Journal of Applied Soft Computing, Elsevier.*

[28] Shi, J., & Malik, J. (2000). Normalized Cuts and Image Segmentation. *IEEE Transactions on Pattern Analysis and Machine Intelligence, 22(8), 888-905.*

[29] Sabor, N., & Abo-Zahhad, M. (2020). A comprehensive survey of intelligent-based hierarchical routing protocols for wireless sensor networks. *In: De D., Mukherjee A., Kumar Das S., Dey N. (eds) Nature Inspired Computing for Wireless Sensor Networks. Springer Tracks in Nature-Inspired Computing, Springer, Singapore, 197-257. https://doi.org/10.1007/978-981-15-2125-6_10*

[30] Soleimani, M., Sharifian, A., & Fanian, A. (2013). An energy-efficient clustering algorithm for large scale wireless sensor networks. *21st Iranian Conference on Electrical Engineering (ICEE), IEEE.*

[31] Sonam, L., Mehfuz, S., Urooj, S., & Alrowais, F. (2020). Fuzzy clustering algorithm for enhancing reliability and network lifetime of wireless sensor netwotks. *IEEE Access, vol.8, 66013-66024.*

[32] Wankhade, N.R., Choudhari, D.N., & Thakre, V.M. (2016). NEEUC: Energy-efficient unequal clustering algorithm for wireless sensor networks. *International Journal of Advanced Research in Computer and Communication Engineering, 5(12), 353-358.*

[33] Yang, Y., Huang, W., & Yuan, H. (2012). An uneven hierarchical clustering o energy balanced strategy for wireless sensor networks. *In Proceedings of ICSP, 1550-1553.*

[34] Zhang, X. (2011). The Laplacian eigenvalues of grahs: a survey. *arXiv: 1111.2897 [math CO]*.

[35] Zhukov, L.E. (2015). Lecture on Graph partitioning algorithms. Retrieved from http://www.leonidZhukov.net/hse/2015/network.